

# Improvements on Dynamic On-State Resistance in Normally-off GaN HEMTs

Carsten Kuring<sup>1</sup>, Marvin Tannhäuser<sup>2</sup>, Sibylle Dieckerhoff<sup>1</sup>

<sup>1</sup> Chair of Power Electronics, Technische Universität Berlin, Germany

<sup>2</sup> Siemens AG, Corporate Technology, Software Defined Inverter, Germany

Corresponding author: Carsten Kuring, carsten.kuring@tu-berlin.de

The Power Point Presentation will be available after the conference.

## Abstract

The use of gallium nitride (GaN) wide-bandgap power semiconductors with small on-state resistance and small parasitic capacitances promises minimized conduction and switching losses in power electronic converters. The increase of the dynamic on-state resistance in normally-off GaN High Electron Mobility Transistors (HEMT) related to charge trapping and hot electron injection directly affects conduction losses and reduces the achievable benefit of GaN devices in power electronics. This paper demonstrates that the extend of dynamic  $R_{on}$ -increase significantly depends on the operation conditions and exemplarily shows recent improvements of commercially available devices.

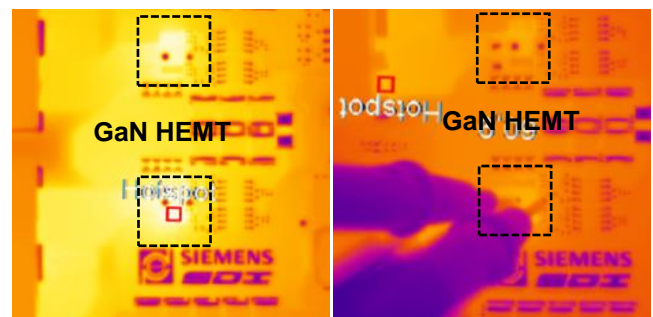
## Introduction

Normally-off power semiconductors are preferred in power electronics due to reduced effort regarding safety concept and start-up strategy, but in case of GaN HEMTs show an increase of the on-state resistance  $R_{on}$  in switched operation [1], [2]. Susceptibility to this dynamic  $R_{on}$ -increase inevitably leads to increased conduction losses [3], and consequently it is mandatory to account for these effects in the design phase of a power electronic converter. The extend of dynamic  $R_{on}$ -increase significantly depends on the semiconductor design [2], [4], [5] and on the operation conditions [6], [7], [8] as well as on the device design.

All presented investigations are based on engineering samples of the EPC2047 normally-off GaN HEMT (200 V, 32 A, 10 m $\Omega$ ) [9]. Initial testing of these devices originating from an early production lot "A" and a newer lot "B" in two identical converter prototypes revealed a noticeable difference in the device temperature despite identical operation conditions (Fig. 1).

In order evaluate these recent achievements in device design, both production lots of the EPC2047 are systematically tested in a half-bridge topology according to their specific on-state characteristic in double-pulse switching tests as well as in pulsed and continuous operation. A wide range of operation conditions is considered in order to depict the impact of selected devices stresses, such as high

blocking voltage or high load current, on the dynamic on-state resistance.



a) Lot "A" of EPC2047, hot-spot at GaN HEMT (90.2°C)      b) Lot "B" of EPC2047, hot-spot at inductor (68.8°C)

Fig. 1: Soft-switching boost converter stage applying two different lots of EPC2047 at identical operation conditions ( $V_{in} = 30$  V,  $V_{out} = 160$  V,  $P_{out} = 300$  W)

## I Test methodology

The characterization of the EPC2047 includes three test scenarios: First, the double-pulse switching test allows for high load current stress, as device heating remains limited.

Second, pulsed operation, reflecting the start-up sequence of continuous operation, reveals interacting effects on the on-state resistance, e.g. de-trapping vs. accumulation of charge trapping [1] and heating. The GaN HEMT half-bridge converter

is operated for approx. 9 ms. Depending on the selected switching frequency (Tab. 1) this covers 450...1800 switching cycles. Although in this operation mode the on-state resistance is increased by charge accumulation and heating, the converter has not achieved thermal steady state. Accordingly, the tested load current is significantly reduced compared to the double-pulse tests but still higher than in continuous operation.

Finally, in continuous operation the half-bridge converter is operated in thermal steady state and exposed to forced air-cooling to increase the load current capability. Nevertheless, the maximum output current is limited by the device temperature and is considerably smaller than in double-pulse switching tests and pulsed operation. Accurate on-state voltage measurement is especially challenging in continuous operation as the on-state voltage is small due to the necessary load current derating. Therefore, the evaluation of continuous operation focusses on the device temperature at different operation conditions.

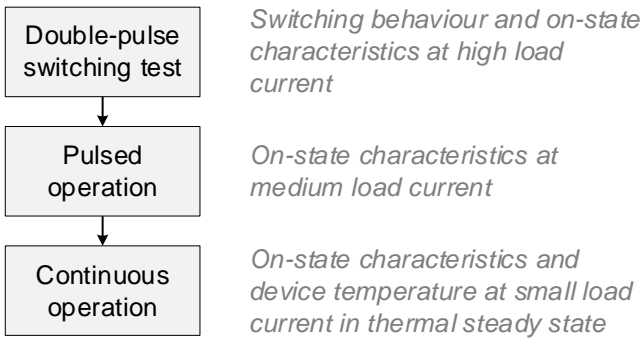


Fig. 2: Covered test scenarios

	Double-pulse test	Pulsed operation	Continuous operation
<b>DC-Link voltage</b> $V_{DC}$ (V)	50...150	50...150	50...150
<b>Load current</b> $I_L$ (A)	20...110	5...25	2.5...7.5
<b>Switching frequency</b> $f_s$ (kHz)	-	50...200 (duty-cycle $D=0.5$ )	50...200 (duty-cycle $D=0.5$ )
<b>Gate resistors</b> $R_{G\ on}/R_{G\ off}$ ( $\Omega$ )	10 / 1.2 6.8 / 0.5 3.0 / 0	3.0 / 0	3.0 / 0

Tab. 1: Investigated parameters affecting on-state characteristics of normally-off GaN HEMTs

In all three test scenarios an inductive load is connected between DC+ and the switching node of the half-bridge (Fig. 3). Accordingly, the investigated bottom-side GaN HEMT experiences hard-switching. The double-pulse tests use a single load inductor  $L = 28\ \mu\text{H}$ . In this part of the investigation the load current is adjusted by the length of the load inductor charging pulse. In pulsed and continuous operation, though, an additional load resistor is connected in series to the load inductor. The load resistance is adjusted to obtain the desired load current at a fixed DC-link voltage while the duty cycle is kept constant (Tab. 1).

## II Extraction of the transient on-state resistance

An accurate on-state voltage measurement requires a measuring range according to the expected transient on-state voltage drop which is commonly significantly lower than the off-state blocking voltage. Therefore, an active clamping circuit disconnects the oscilloscope from the switching node when the bottom-side GaN HEMT  $T_{bot}$  is in blocking state. This approach prevents the oscilloscope input amplifier from saturation or even damage (Fig. 3).

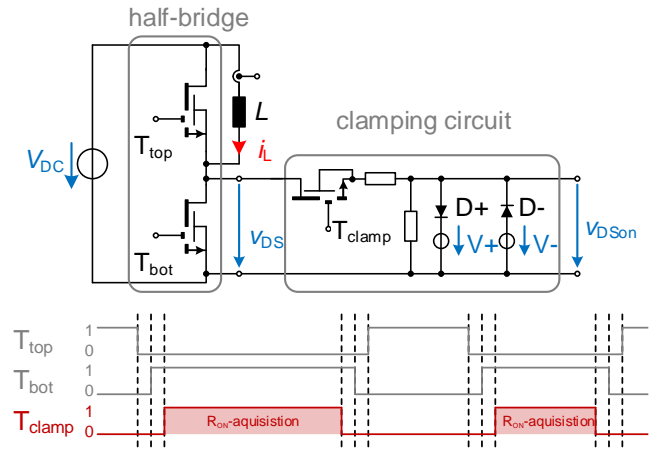


Fig. 3: Test setup with clamping circuit and control scheme

The clamping circuit is optimized for sensing small on-state voltages  $R_{on} \cdot I_D$ , but its parasitic capacitance leads to higher capacitive turn-on losses in  $T_{bot}$ . However, the impact remains limited as the clamping transistor  $T_{clamp}$  has a much smaller parasitic output capacitance than the EPC2047 transistors ( $C_{O,ER} = 22\ \text{pF}$ , [10] vs.  $450\ \text{pF}$ , [9]). Due to the necessary deadtimes of the actively controlled clamping circuit, the on-state voltage is recorded

starting approx. 40 ns after the turn-on of the investigated bottom-side transistor  $T_{\text{bot}}$ . The transient on-state resistance of  $T_{\text{bot}}$  is then calculated by means of the on-state voltage  $v_{\text{DSon}}$  and the load current  $i_L$  (Fig. 4). To enable an analysis of a large number of double-pulse switching tests, averaged on-state resistance values  $R_{\text{on a}}$  (before hard turn-off at  $t=0 \mu\text{s}$ ) and  $R_{\text{on b}}$  (after hard turn-on at  $t=2 \mu\text{s}$ ) are derived from each transient on-state resistance (Fig. 4). The applied averaging window for  $R_{\text{on a}}$  as well as  $R_{\text{on b}}$  is  $t_{\text{avg}}=0.5 \mu\text{s}$ . During blocking-state of  $T_{\text{bot}}$  and  $T_{\text{Clamp}}$  the calculated  $R_{\text{on}}$  is neglected.

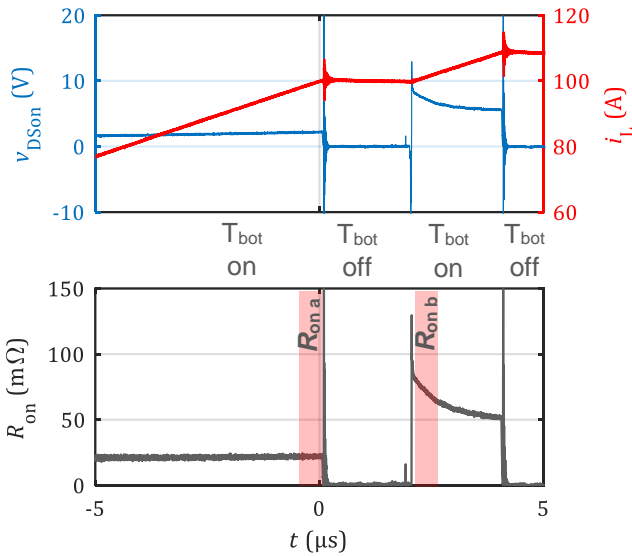


Fig. 4: Extraction of transient and average on-state resistance in double-pulse switching test

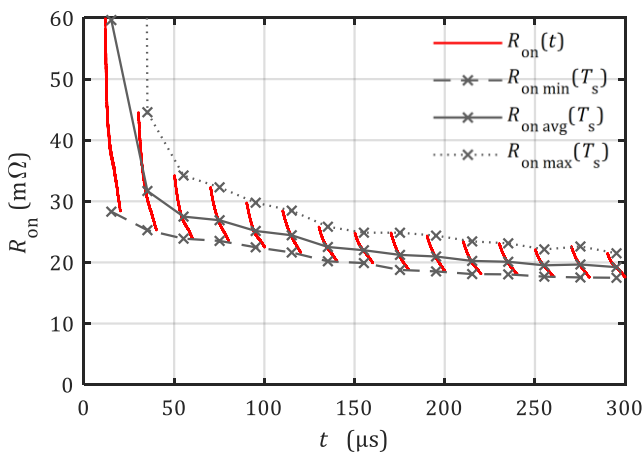


Fig. 5: Extraction of the cycle-by cycle on-state resistance values in pulsed operation

The on-state characterization in pulsed operation also relies on the clamping circuit for extraction of

the on-state voltage. Accumulation of charge traps, detrapping and heating affect the on-state characteristics and introduce time constants of several switching periods (Fig. 5). In contrast, the transient on-state resistance during each on-state period can show significantly faster characteristics. To enable a long-term evaluation of the on-state resistance over several switching periods in the ms-range, the maximum, average and minimum on-state resistance ( $R_{\text{on max}}$ ,  $R_{\text{on avg}}$ ,  $R_{\text{on min}}$ ) is calculated for each on-state period.

### III Dynamic on-state characteristics in double-pulse test setup

The parasitic capacitance introduced by the clamping circuit (Fig. 3) slightly increases the parasitic capacitance of the switching node and consequently affects the switching characteristics. Therefore, initial switching characterization of both device lots A and B in the double-pulse test uses a conventional single-ended passive probe without clamping circuit.

#### Switching characteristics

The GaN HEMT achieves fast switching with slew rates up to 100 V/ns for turn-off and 40 V/ns for turn-on depending on the load current and the applied gate resistors. The turn-off voltage slew rate in Fig. 6 ( $dv/dt > 0$ ) increases with the load current, because after turn-off of the bottom-side transistor, the load current charges the output capacitance of the half-bridge. Consequently, a larger load current results in faster charging and hence shorter voltage rise times.

At load currents  $i_L < 40$  A, the turn-off voltage slew rate is independent from the size of the turn-off gate resistor for both investigated lots of the EPC2047. However, lot B achieves marginally lower turn-off voltage slew rates.

Considering higher load currents  $i_L > 40$  A, the turn-off voltage slew rate is increased with decreasing turn-off gate resistor due to reduced feedback on the gate-source voltage through the Miller capacitance. Note that at load currents  $i_L > 70$  A, lot B achieves higher turn-off voltage slew rates compared to lot A.

Regarding turn-on, the switching speed decreases with the turn-on gate resistance as well as with the load current. Furthermore, lot B achieves noticeably faster turn-on compared to lot A. This effect probably results from a lower on-state resistance of lot B directly after turn-on as shown in Fig. 7...Fig. 9. Nevertheless, further possible root

causes are e.g. a reduced parasitic gate resistance or a smaller Miller capacitance  $C_{GD}$  of lot B.

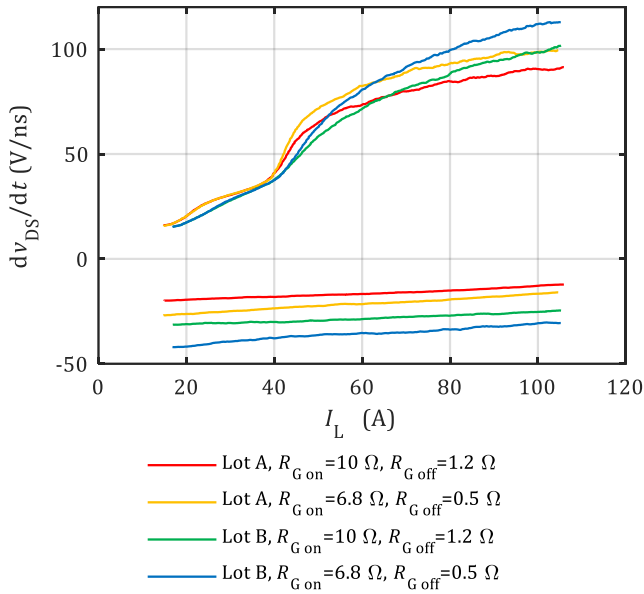


Fig. 6: Drain-source voltage slew rate during turn-off ( $d v / d t > 0$ ) and turn-on ( $d v / d t < 0$ )

### Impact of load current

In the double-pulse test, the bottom-side GaN HEMT is initially in off-state and susceptible to charge trapping contributing to an increased on-state resistance after turn-on. Furthermore, during turn-on, high current density and high electric field strength occur simultaneously in the GaN HEMT and lead to hot electron injection [11]. In addition to charge trapping effects, this results in a further increase of the on-state resistance. Consequently, the load current and switching speed as well as the blocking conditions, such as blocking voltage and blocking duration have impact on the on-state characteristics.

The measurements in Fig. 7 exemplarily depict the transient on-state resistance (hard turn-off at  $t = 0\ \mu\text{s}$  and hard turn-on at  $t = 1.04\ \mu\text{s}$ ).

The on-state resistance of the investigated normally-off GaN HEMTs significantly varies between both production lots. Lot A achieves a  $R_{\text{on}}$  of approx.  $23\ \text{m}\Omega$  before blocking ( $t < 0\ \mu\text{s}$ ), while lot B has a much lower resistance complying with the datasheet ratings of  $7\ \dots\ 10\ \text{m}\Omega$  [9].

Besides that, both production lots experience an increased  $R_{\text{on}}$  after the hard turn-on. The extend of dynamic  $R_{\text{on}}$ -increase ( $R_{\text{on}b} - R_{\text{on}a}$ ) rises with the load current even though the DC-link voltage is kept constant in Fig. 7. Furthermore, the device of lot A shows a short and fast decaying peak on-

state resistance at  $I_L = 100\ \text{A}$  right after turn-on which is not present in case of lot B.

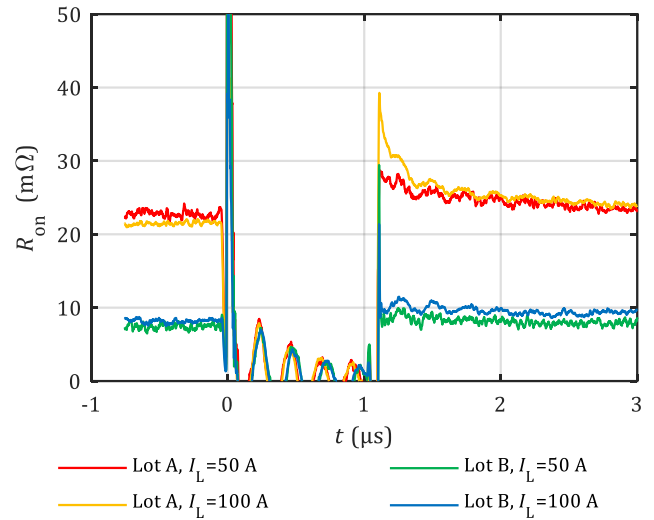


Fig. 7: Transient on-state resistance in double-pulse switching test for different load currents ( $V_{DC} = 100\ \text{V}$ ,  $R_{G\text{on}} = 6.8\ \Omega$ ,  $R_{G\text{off}} = 0.5\ \Omega$ )

### Impact of blocking voltage stress

High blocking voltage stress is further contributing to dynamic on-state characteristics of normally-off GaN transistors in switched operation. The average on-state resistance in Fig. 8 shows a significant difference of  $R_{\text{on}}$ -increase ( $R_{\text{on}a}$  vs.  $R_{\text{on}b}$ ) between the investigated production lots. Assuming a constant load current, the on-state resistance before as well as after blocking noticeably rises with the blocking voltage for lot A, whereas in case of lot B the effect remains strongly limited.

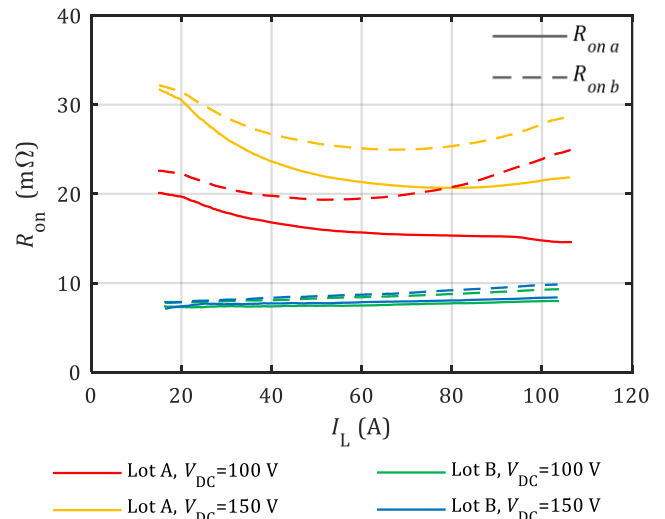


Fig. 8: Average on-state resistance in double-pulse switching test for different DC-link voltages and load currents ( $R_{G\text{on}} = 6.8\ \Omega$ ,  $R_{G\text{off}} = 0.5\ \Omega$ )

The on-state resistance  $R_{on a}$  of lot A decreases with the load current until  $I_L \approx 80$  A. In our measurements the load inductor is kept constant and an increasing length of the first charging pulse is needed to increase the load current. Due to increased pulse length and hence increased detrapping time, the average on-state resistance  $R_{on a}$  of lot A is reduced for high load currents. Heating of the GaN HEMT during the charging pulse has an inverse effect so that the on-state resistance  $R_{on a}$  for  $I_L > 80$  A increases again for lot A. In contrast, the on-state resistance of lot B monotonously rises with the load current due to heating and exhibits no local minimum caused by detrapping effects.

The absolute  $R_{on}$ -increase  $R_{on b} - R_{on a}$  after hard-switching events rises with the load current for both production lots and DC-link voltages. However, lot B achieves much lower on-state resistance values ( $R_{on a}$ ,  $R_{on b}$ ) as well as a reduced extend of  $R_{on}$ -increase, indicating a significantly improved robustness towards charge trapping effects.

### Impact of switching speed

The switching speed of the investigated GaN HEMT is effectively adjusted by applying different pairs of gate resistors (Fig. 6).

Fig. 9 depicts the effect of switching speed on the  $R_{on}$  under clamped inductive switching conditions. Fast switching achieved by small gate resistors noticeably reduces the on-state resistance after blocking ( $R_{on b}$ ) for lot A, leading to reduced conduction losses in continuous operation, if stable switching is guaranteed.

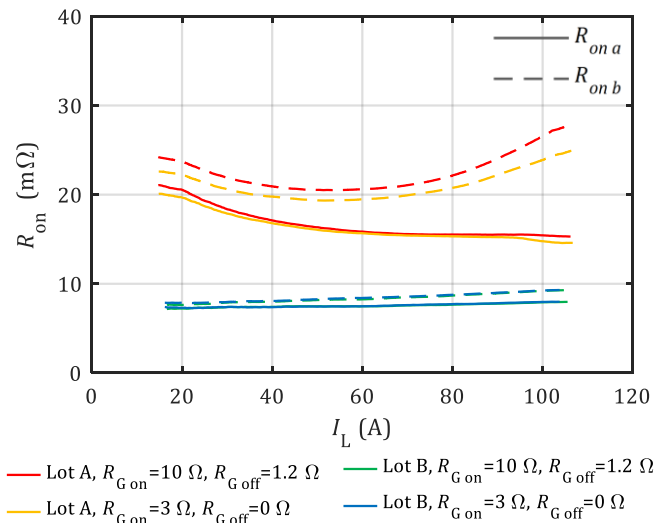


Fig. 9: Average on-state resistance in double-pulse switching test for varying gate resistors and load currents ( $V_{DC} = 100$  V)

In case of lot B the on-state resistance remains unaffected for the considered gate resistor configurations. Due to the significantly reduced impact of the switching speed on the dynamic  $R_{on}$ , the selection of the gate resistors is no longer restricted by the demand for fastest possible switching to minimize the dynamic  $R_{on}$ -increase.

In summary, the double-pulse switching test has verified that the dynamic on-state resistance rises with the load current and blocking voltage for both lots of the EPC2047. However, lot B demonstrates a significantly improved robustness to dynamic  $R_{on}$ -increase.

## IV Dynamic on-state characteristics in pulsed operation

The pulsed operation resembles the start-up sequence of a continuous operation scenario. Similar to a real-world power electronic application, the investigated bottom-side transistor is initially in blocking state and susceptible to charge trapping.

### Impact of load current

Measurements of the on-state resistance in pulsed operation in Fig. 10 depict a partial recovery from charge trapping effects resulting in a temporary minimum of the on-state resistance within the first millisecond of operation.

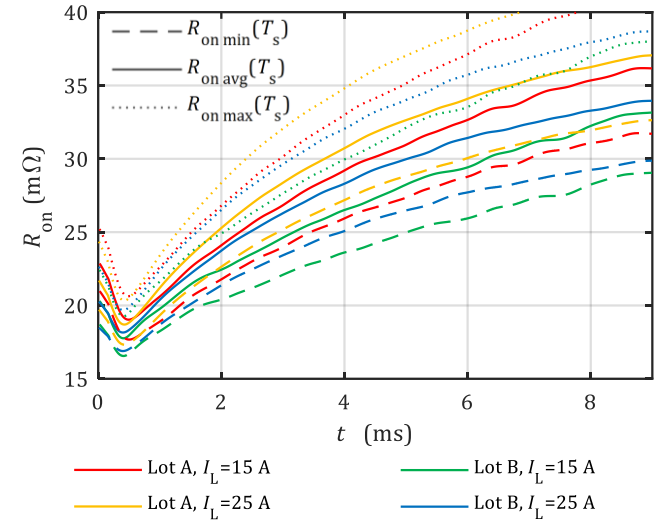


Fig. 10: On-state resistance in pulsed operation for different load currents ( $V_{DC} = 150$  V,  $f_s = 100$  kHz, 900 switching cycles,  $D = 0.5$ )

The average on-state resistance  $R_{on avg}(T_s)$  and its range  $\Delta R_{on}(T_s) = R_{on max}(T_s) - R_{on min}(T_s)$  during on-state  $D \cdot T_s$  then increase with time due to accumulation of charge trapping and heating of the GaN

HEMT. The  $R_{on}$  rises with the load due to increased conduction losses, heating during on-state as well as hot electron injection during the switching events.

Assuming a load current  $I_L = 25$  A, lot A achieves an average cycle-by-cycle on-state resistance of 37 m $\Omega$  after 9 ms of operation compared to 34 m $\Omega$  in case of lot B. Although this is still a noticeably benefit margin using lot B, this improvement in pulsed operation is significantly lower than previously indicated by the on-state measurements in the double-pulse switching test (Sec. III).

### Impact of DC-link voltage

Varying the DC-link in pulsed operation reveals a significant shift of the on-state characteristic for both lots of the EPC2047 with increased blocking voltage stress (Fig. 11).

Initially the on-state resistance decays during the first switching cycles due to detrapping regardless of the applied DC-link voltage. In case of the  $V_{DC} = 150$  V,  $R_{on}$  achieves a minimum value at  $t \approx 0.5$   $\mu$ s followed by a strong increase for both investigated lots.

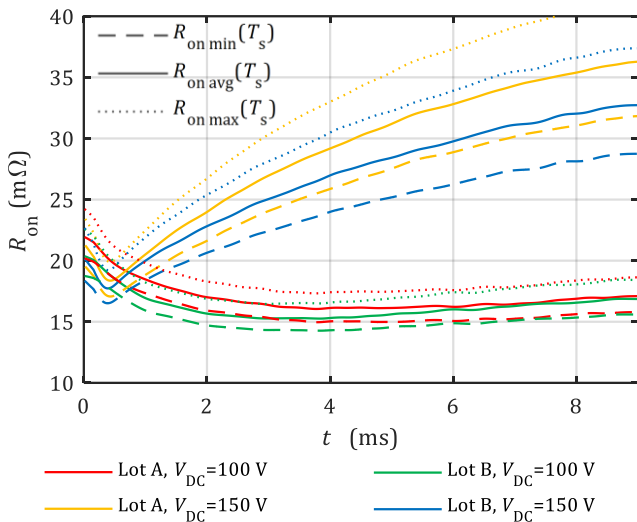


Fig. 11: On-state resistance in pulsed operation for different DC-link voltages ( $I_L = 20$  A,  $f_s = 100$  kHz,  $D = 0.5$ )

Applying a reduced blocking voltage  $V_{DC} = 100$  V, the  $R_{on}$  subsides until  $t \approx 4$  ms when it starts to rise slowly again. Note that at  $V_{DC} = 100$  V lot B shows a slightly faster  $R_{on}$ -decay but after 9 ms of operation both lots achieve a similar on-state resistance.

Although the results in Fig. 11 do not allow for exact separation of charge trapping effects and heating as root cause of  $R_{on}$ -increase, they still demonstrate the extensive impact of blocking voltage stress and emphasize the need of voltage derating in continuous operation.

### Impact of switching frequency

Operating normally-off GaN HEMTs at increased switching frequency inevitable leads to increased switching and conduction losses simultaneously, as the dynamic on-state characteristic exhibits time constants in the  $\mu$ s-range or even above (Fig. 7 vs. Fig. 12).

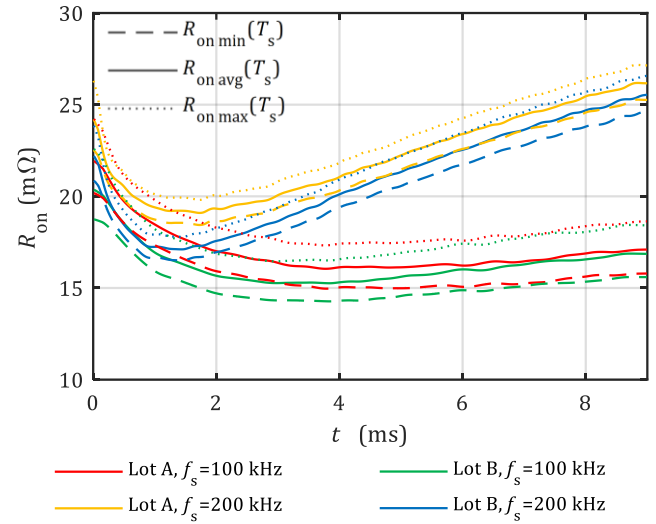


Fig. 12: On-state resistance in pulsed operation for different switching frequencies ( $V_{DC} = 100$  V,  $I_L = 25$  A,  $D = 0.5$ )

The measurement results in Fig. 12 depict the  $R_{on}$  of lot A and lot B for switching frequencies of 100 kHz and 200 kHz in pulsed operation. Again, the tested GaN HEMTs initially recover from trapping effects resulting in a decrease of the on-state resistance followed by  $R_{on}$ -increase resulting from accumulation of charge trapping, hot electron injection and heating. The following  $R_{on}$ -increase is significantly stronger for the higher switching frequency. Dynamic  $R_{on}$ -increase caused by hot electron injection occurring once in a switching cycle during turn-on directly scales with the applied switching frequency. However,  $R_{on}$ -increase due to charge trapping during blocking is much more complex. Increasing the switching frequency at constant duty cycle reduces both, the off-state duration when charge traps build up as well as the on-state time acting as detrapping period. Accordingly, selection of the switching frequency is especially critical when normally-off GaN HEMTs are employed.

In our setup the average load current as well as the load impedance are kept constant for different switching frequencies. This leads to a reduced load current ripple at a higher switching frequency. In accordance to the switching tests from Sec. III, the range of the on-state resistance within a

switching cycle  $\Delta R_{on}(T_s) = R_{on\ max}(T_s) - R_{on\ min}(T_s)$  is therefore reduced for a reduced load current ripple and an increased switching frequency, respectively.

The pulsed operation tests demonstrate the severe impact of high blocking voltage as well as high switching frequencies on the on-state characteristics of the investigated normally-off GaN HEMTs. The load current affects the on-state resistance as well, but the extend of  $R_{on}$ -increase is limited for the considered load current range as long as the GaN HEMTs are operated at reasonable small blocking voltage and switching frequency.

## V Dynamic on-state characteristics in continuous operation

The maximum load current in continuous operation is thermally limited due to the bottom-side cooling concept of the applied GaN HEMTs. Assuming the DC-link voltages and switching frequencies (Tab. 1), a load current up to  $I_L = 5$  A for lot A and up to  $I_L = 7.5$  A for lot B is tested at different switching frequencies and DC-link voltages.

Due to these relatively small load currents, the measured transient on-state voltage is small as well. This results in a reduced measurement accuracy regarding the on-state resistance in comparison to the double-pulse switching test and pulsed operation. Accordingly, the measurement results for the maximum achievable output current (5 A and 7.5 A, respectively) are presented in Fig. 13. Instead, Fig. 14 shows the case surface temperature of the bottom-side GaN HEMT for all considered operation conditions.

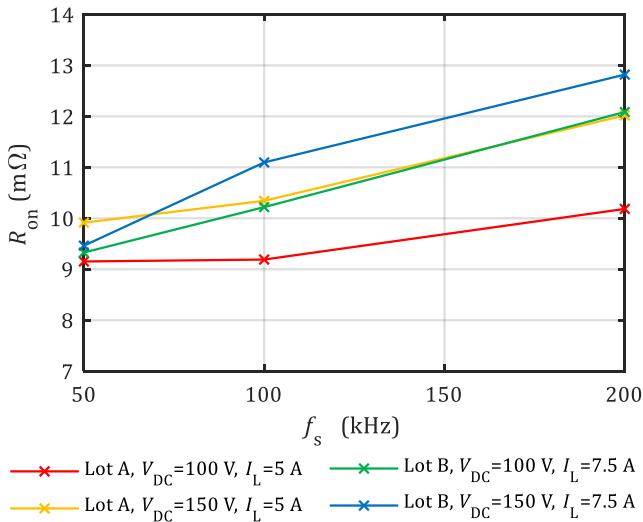


Fig. 13: Average on-state resistance in continuous operation

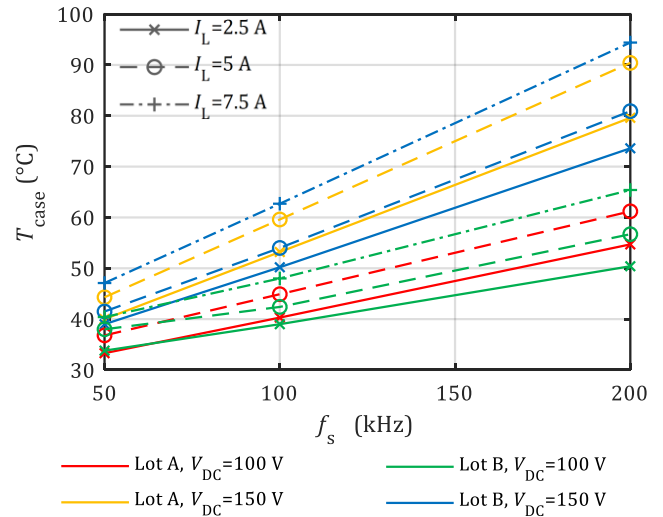


Fig. 14: Case temperature in continuous operation

As previously indicated by the pulsed operation and the double-pulse tests, the on-state resistance as well as case temperature rise with the applied current, DC-link voltage and switching frequency.

In our investigation a fixed deadtime of 100 ns is applied for the top-side GaN transistor. During the deadtime, the high reverse voltage drop in off-state typical for normally-off GaN HEMTs ( $V_{SD} = 2.2...2.7$  V [9]) results in increased conduction losses contributing to the overall losses of the half-bridge. Therefore, optimized deadtimes could enable reduced conduction losses for the top-side transistor and an increased maximum load current compared to our measurements.

## Conclusion

State-of-the-art commercial normally-off GaN HEMTs still show increased conduction losses in switched operation due to dynamic on-state characteristics. The extend of dynamic  $R_{on}$ -increase significantly depends the operation conditions and the device design.

High load currents and blocking voltage stress lead to an increased on-state resistance in switched operation. Depending on the specific device characteristics, fast switching of GaN-HEMTs can minimize the dynamic  $R_{on}$ -increase and the conduction losses respectively.

Systematic characterization and comparison of two production lots of the EPC2047 have validated continuous improvements in the device technology. Although recent normally-off GaN transistors still exhibit limited dynamic on-state characteristics, the susceptibility towards trapping effects and dynamic  $R_{on}$ -increase respectively, has been significantly reduced.

However, in pulsed and continuous operation the benefit margin of the improved device lot was not as high as indicated by the double pulse tests. Due to the significant  $R_{on}$ -increase caused by charge accumulation and heating, characterization of normally-off GaN-HEMTs in pulsed and continuous operation is mandatory. Furthermore, these effects need to be accounted in the device models to enable meaningful converter simulation.

Finally, in continuous operation, the investigated bottom-side cooled normally-off GaN HEMTs are thermally limited and need to be operated significantly below their electrical ratings. Thermal device management of GaN power transistors is especially critical, as they achieve a significantly higher loss density compared to conventional Si power semiconductors. Therefore, advanced packaging accounting for the specific demands of GaN power semiconductors need be developed. This includes optimization of the thermal interfacing as well as minimization parasitic circuit elements.

## Acknowledgement

Efficient Power Conversion Corporation supported this work by supplying the investigated lot B of the EPC2047 GaN HEMTs.

## References

- [1] J. Böcker, C.Kuring, M.Tannhäuser and S. Dieckerhoff, "Ron Increase in GaN HEMTs – Temperature or Trapping Effects".*Conf. Proc. of the IEEE/ECCE2017*.
- [2] J. Würfl, E. Bahat-Treidel, O. Hilt, M. Troppenz, M. Wolf, J. Böcker, C. Kuring and S. Dieckerhoff, "Dynamic drift effects in GaN power transistors: Correlation to device technology and mission profile," *Conf. Proc. IEEE/IPEC*, 2018.
- [3] C.Kuring, J. Lenth, J. Böcker, T. Kahl and S. Dieckerhoff, "Application of GaN-GITs in a Single-Phase T-Type-Inverter," *Conf. Proc. of the PCIM Europe*, 2018.
- [4] M. Uren, J. Möreke and M. Kuball, "Buffer Design to Minimize Current Collapse in GaN/AlGaN HFETs," *IEEE Transactions on Electron Devices*, Vol. 59, No. 12, 2012.
- [5] W. Saito, T. Nitta, Y. Kakiuchi, Y. Saito, K. Tsuda, I. Omura and M. Yamaguchi, "Suppression of Dynamic On-Resistance Increase and Gate Charge Measurements in High-Voltage GaN-HEMTs With Optimized Field-Plate Structure," *IEEE Transactions on Electron Devices*, Vol. 54, No. 8, 2007.
- [6] N. Badawi, O. Hilt, E. Baht-Treidel, J. Böcker, J. Würfl and S. Dieckerhoff, "Investigation of the Dynamic On-State resistance of 600 V Normally-Off and Normally-On GaN HEMTs," *IEEE Transactions on Industry Applications*, Vol. 52, No. 6, 2016.
- [7] C. Kuring, O. Hilt, J. Böcker, M. Wolf, S. Dieckerhoff and J. Würfl, "Novel monolithically integrated bidirectional GaN HEMT".*Conf. Proc. of the IEEE/ECCE2018*.
- [8] N. Badawi and S. Dieckerhoff, "A new Method for Dynamic Ron Extraction of GaN," *Conf. Proc. of the PCIM Europe*, 2015.
- [9] EPC - Efficient Power Conversion, "EPC2047 – Enhancement-Mode Power Transistor - Preliminary Specification Sheet," 2018.
- [10] GaN Systems, „GS66502B, Bottom-side cooled 650 V E-mode GaN transistor, Preliminary Datasheet, Rev. 181214“.
- [11] F. Yang, C. Xu and B. Akin, "Experimental Evaluation and Analysis of Switching Transients's Effects on Dynamic On-Resistance in GaN HEMTs," in *IEEE Transactions on Power Electronics*, 2019.